Open Access

Recent Progress in Materials

LIDSEN Publishing Inc.

Original Research

Valorization of Agroindustrial Waste as Biosorbent of Lead (II) in Solution and its Reuse in the Manufacture of Building Bricks

Melisa S. Romano *, Valeria Corne, Ricardo R. Azario, Emiliano Centurión, María del Carmen García

Grupo de Investigación en Química y Ambiente, Universidad Tecnológica Nacional (UTN-FRCU), Argentina; E-Mails: romanom@frcu.utn.edu.ar; cornev@frcu.utn.edu.ar; azarior@frcu.utn.edu.ar; emilianocenturion96@gmail.com; garciam@frcu.utn.edu.ar

* **Correspondence:** Melisa S. Romano; E-Mail: romanom@frcu.utn.edu.ar

Academic Editor: Riyadh Al-Ameri

Special Issue: Recycling and Reuse of Waste Materials in Construction

Recent Progress in Materials
2025, volume 7, issue 1
doi:10.21926/rpm.2501002

Received: October 24, 2024
Accepted: January 02, 2025
Published: January 10, 2025

Abstract

Lead is a non-biodegradable toxic heavy metal. Biosorption is a simple, cost-effective and eco-friendly method for remediating lead-contaminated environments. Additionally, rice husk is a highly available residual biomass that can be used as a biosorbent. This study aimed to analyze the biosorption of Pb^{2+} using both natural and chemically treated rice husk and to evaluate the incorporation of the resulting biomass-contaminant residue into ceramic matrices to immobilize the removed Pb^{2+}. Natural and alkaline-activated rice husks were characterized and used as biosorbents for Pb^{2+} in solution. Experimental results demonstrated that the maximum removal occurred at pH 5 and equilibrium was reached in 30 minutes. The chemical modification caused a significant increase in the removal efficiency, from 7.08 ± 0.59% to 94.51 ± 1.17% at room temperature and a biosorbent dosage of 3 g/L. The Langmuir isotherm model was the most appropriate for representing Pb^{2+} biosorption onto rice husk. The maximum adsorption capacities (q_m, mg/g) were 8.464 for natural rice husk and 27.450 for the chemically modified form. Biosorption data followed a pseudo-second-order kinetic model. Ceramic pieces were prepared by mixing commercial clay and rice husk containing adsorbed Pb^{2+}, with the residue added at 10% by volume. Pb^{2+} fixation was assessed through

ecotoxicity and leaching tests, which confirmed that ceramic pieces immobilized Pb^{2+} within their structure. In conclusion, the use of alkaline-treated rice husk as a Pb^{2+} biosorbent, combined with the incorporation of the biomass-Pb^{2+} residue into ceramic matrices for Pb^{2+} immobilization, provides an eco-friendly alternative for detoxifying lead-contaminated environments.

Keywords
Biosorption; Pb^{2+}; rice husk; building bricks

1. Introduction

Drinking water standards and the quality of wastewater discharged into rivers, seas and other open water bodies are among the major global environmental issues [1]. Agrochemicals, pharmaceuticals, petroleum products, heavy metals, and other organic and inorganic compounds contribute to water pollution [2, 3]. These pollutants adversely affect aquatic environments and present serious risks to both humans and animals [3].

Heavy metals are among the most hazardous water contaminants due to their toxic effects on human health and the environment [2-5]. These elements are released into water bodies from both natural and anthropogenic sources, and in some cases, their levels in surface water exceed the maximum permissible values for drinking water [6]. Furthermore, these toxic metals are non-biodegradable and tend to bioaccumulate and biomagnify through the food chain [4, 7].

Lead is a typical heavy metal pollutant found in wastewater and aquatic environments due to industrial activities such as mining, smelting, metallurgy, battery manufacturing, metal plating, and finishing, among others [4, 8-12]. This toxic substance can adversely affect various physiological systems, including nervous, immune, reproductive, and cardiovascular [13]. Consequently, strict regulations on lead levels in water are essential. The US Environmental Protection Agency (US EPA) has established a maximum contaminant level (MCL) for lead in drinking water, setting the threshold at 0.015 mg/L [11].

Several technologies have been developed to address this environmental challenge [14-18]. Among these, the biosorption process offers advantages such as high efficiency, cost-effectiveness, and the versatility of using natural materials as biosorbents [19, 20]. Additionally, agricultural waste has become a valuable biomass source for these processes [21-25].

Rice husk, a significant agricultural by-product in the eastern region of Argentina, is an attractive bio-based adsorbent material for pollutant removal [26, 27]. It contains high proportions of compounds such as cellulose, hemicellulose, lignin, and silica, which provide binding sites capable of retaining metals [28]. Therefore, this context presents a compelling case for utilizing this waste in the eco-friendly and cost-effective detoxification of lead-contaminated environments.

The biosorption process produces a biomass-contaminant residue, making it important to consider a viable and low-cost strategy for its final disposal. A novel alternative to this issue involves reusing these adsorbent-pollutant wastes in ceramic materials [29]. This addition becomes a pore-former by generating gases and inorganic compounds at the combustion temperatures inside the brick, resulting in lighter bricks, as demonstrated in several agricultural biomass studies [29-31].

In this context, this study aimed to evaluate the Pb^{2+} removal capacity of rice husk while optimizing the physicochemical parameters governing this process. Additionally, the feasibility of incorporating the Pb^{2+}-contaminated rice husk residue into clay ceramic matrices to immobilize the removed Pb^{2+} was assessed. This approach mitigates the environmental impact commonly associated with biosorption processes.

2. Materials and Methods

2.1 Biosorbents Preparation and Characterization

Two biosorbents, described below, were prepared from rice husk obtained from a rice mill in Entre Ríos, Argentina.

Natural rice husk (NRH): Rice husk was washed with distilled water to remove residues and then dried in an oven at 80°C for subsequent storage.

Alkaline-activated rice husk using potassium hydroxide (KOH-RH): Natural rice husk was mixed with 1% m/m KOH and boiled for 30 min. The mixture was left overnight, filtered, washed with distilled water and 1 M HCl to reach pH 5, and dried at 100°C in an oven for 24 h.

The rice husk was characterized in a previous study [29]. Additionally, the pH at the point of zero charge (pH_{PZC}) for both NRH and KOH-RH was determined using the immersion technique, as described by Fiol & Villaescusa [32].

2.2 Adsorbate Preparation

A stock solution of Pb^{2+} was prepared by dissolving an appropriate amount of $Pb(NO_3)_2$ in distilled water. Serial dilutions were then performed to obtain synthetic wastewater with the desired Pb^{2+} concentration. Solutions of 1 M NaOH and 1 M HCl adjusted the pH. All chemicals used were of analytical grade.

2.3 Biosorption Experiments

Biosorption tests were conducted under batch conditions at 20 ± 4°C. The influence of biosorbent dosage (1–50 g/L), pH (1-6), contact time (1-180 min), and initial Pb^{2+} concentration (10-400 mg/L) were evaluated. After the biosorption experiments, samples were filtered and the residual Pb^{2+} in solution was quantified by atomic absorption spectroscopy (Buck 210 VGP, USA) at 283.3 nm. The removal percentage was calculated using the following equation (Eq. 1):

$$\% \, Pb^{2+} \, biosorption = \frac{C_i - C_e}{C_i} \cdot 100\% \quad (1)$$

Where C_i (mg/L) is the initial concentration and C_e (mg/L) is the equilibrium concentration of Pb^{2+} ions.

The amount of metal retained in the biosorbent (q_e) was calculated from the experimental data using equation 2 (Eq. 2):

$$q_e = V \cdot \frac{C_i - C_e}{m} \quad (2)$$

Where *V* is the volume of solution (L) and *m* is biosorbent mass (g).

The results are expressed as the mean ± standard error of the mean (n = 3). Statistical analysis was performed using Student's *t*-test or one-way analysis of variance (ANOVA) followed by Dunnett's test. In all cases, $p < 0.05$ was considered statistically significant.

The obtained biosorption data were analyzed to study the equilibrium and kinetic of the process. Data were fitted to Lagergren pseudo-first-order and pseudo-second-order equations. Pb^{2+} biosorption equilibrium was modeled by using Langmuir, Freundlich and Dubinin-Radushkevich models.

2.4 Ceramic Bricks Design and Manufacture

The ceramic brick manufacturing process was designed based on the properties of the commercial clay used and the thermal behavior of the rice husk.

After the sorption tests, NRH and KOH-RH samples loaded with Pb^{2+} were grinding and sieving to obtain a particle size less than 1 mm.

Ceramic bricks were prepared by mixing commercial clay with either NRH or KOH-RH (with or without adsorbed metal) at 10% by volume [33]. For comparison, a sample of commercial clay with no added residue was also prepared. The mixtures were compacted into molds (70 mm × 40 mm) using uniaxial pressure at 25 MPa, with 8% by weight of water added, resulting in bricks approximately 15 mm thick. After a drying period, the samples were thermally treated at 1000°C using heating curves similar to those used in the ceramic industry.

2.5 Characterization of Compact Bodies

The ceramic products were characterized using several techniques, including porosity (P), modulus of rupture (MOR), permanent volumetric variation (PVV), weight loss on ignition (LOI), and mechanical properties. The porosity and water absorption of the samples were determined following ASTM C20-00 standards. The modulus of rupture was measured using a Digimess Model TG100L machine, with a maximum capacity of 500 kg and a test speed of 0.5 mm/min. The PVV and LOI values were calculated by measuring the dimensions (length, width, and thickness) and the weight of each sample before and after sintering at 1000°C.

2.6 Immobilization Studies

To assess the immobilization of the toxic metal in the clay matrix, ecotoxicity and leaching tests were performed on the samples. Both the KOH-RH loaded with adsorbed Pb^{2+} and the ceramic brick containing the contaminated husk replacement were tested.

In the ecotoxicity test (IRAM 29114, Argentina), the initial elutriate was prepared by suspending the residue in distilled water at a 1:4 ratio, stirring for 2 h, and filtering. The experiments were performed in triplicate using concentrations of 6, 12, 25, 50, and 100% of the initial elutriate. Twenty seeds of ryegrass were placed in 90 mm Petri dishes, between two filter papers, and 3.5 mL of the solution to be evaluated was added. The dishes were covered and incubated at 24°C for 120 h. Reference controls were performed with distilled water. The evaluation points included the number of germinated seeds and the radicle elongation, which was expressed as a percentage of inhibition relative to the control samples with distilled water. Evaluating the elongation of the seedling radicle

measures the toxic effects of soluble compounds present at low concentrations, which might not inhibit germination but can delay or inhibit entirely radicle elongation.

The leaching characterization of the contaminated rice husk and bricks followed EPA standard 1310. An appropriate amount of rice husk or brick blocks was stirred with the extraction solvent for 24 hours. The liquid used was 16 times the weight of the solid. Finally, the systems were filtered, and Pb^{2+} concentration was determined by atomic absorption spectroscopy.

3. Results and Discussion

3.1 Rice Husk Characterization

NRH and KOH-RH characterization was previously described [29]. Briefly, semi-quantitative chemical analysis by EDS of NRH showed that biomass contains high percentages of carbon, oxygen, and silica. The materials have a suitable morphological profile to retain metal ions, as revealed by SEM images. XRD patterns of NRH and KOH-RH exhibit peaks corresponding to a crystal structure of cellulose and amorphous silica. FT-IR spectra of NRH and KOH-RH did not differ significantly. These materials exhibit –Si–OH, –OH, –Si–O–Si– and carbonyl bands that might participate in metal biosorption. DTA-TGA profiles corresponding to NRH and KOH-RH show several exothermic peaks, which have been assigned to the biopolymers present in the biomass. The peak assigned to lignin is shifted toward higher temperatures in the DTA-TGA curve of KOH-RH, suggesting that the alkali treatment makes the material structure more resistant.

The pH_{PZC} determination for the biosorbents is summarized in Figure 1. The pH_{PZC} values were 6.36 and 7.71 for NRH and KOH-RH, respectively. At solution pH values lower than pH_{PZC}, the biosorbent surface becomes positively charged, reducing the electrostatic attraction of cationic species under investigation. Conversely, at solution pH values higher than pH_{PZC}, the negatively charged surface of biosorbents facilitates electrostatic interactions between biosorbent and adsorbate.

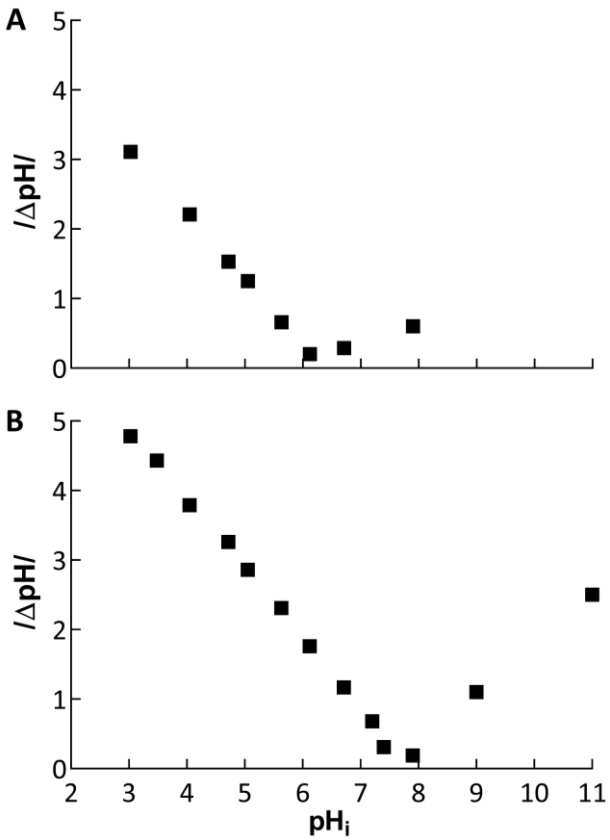

Figure 1 Determination of pH_{PZC}. A: NRH and B: KOH-RH.

3.2 Optimization of Biosorption Parameters Using NRH and KOH-RH

Initially, for the unmodified and chemically treated material, the effect of the mass on Pb^{2+} removal was analyzed. Biosorbent dosage between 1-50 g/L was studied (Figure 2).

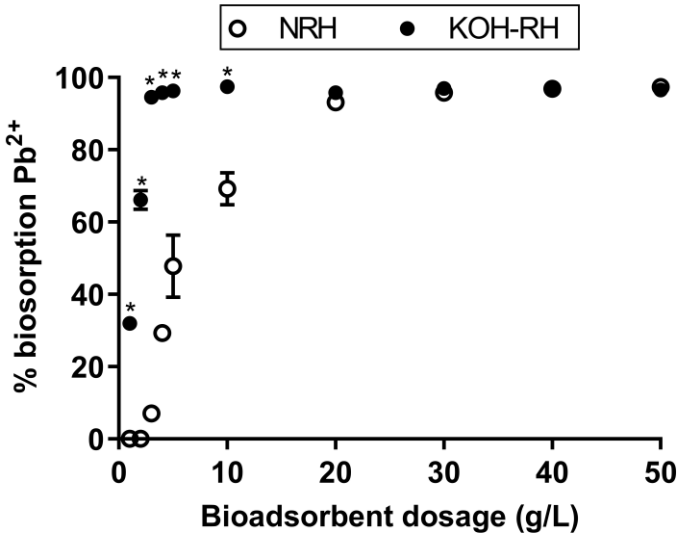

Figure 2 Effect of biosorbent dosage on Pb^{2+} removal by NRH and KOH-RH. Conditions: pH = 5, temperature 20 ± 4°C, time = 1 h and $[Pb^{2+}]_0$ = 50 mg/L. *p < 0.05 vs. the corresponding value in NRH.

The removal of Pb^{2+} by NRH was less than 20% for biosorbent dosages between 1 and 4 g/L. However, at biosorbent dosage higher than 10 g/L, a significant increase in the removal percentage was observed, with the best results achieved for dosages between 20 and 50 g/L. The analysis of the values obtained for KOH-RH showed higher removal efficiency than the untreated material, achieving removal percentages close to 94% when the biosorbent dosage was equal to or greater than 3 g/L. Although the natural husk has proven an effective adsorbent for Pb^{2+} removal in aqueous solution, pre-treatment with potassium hydroxide improved its biosorption capacity. Alkaline modification of the material resulted in a substantial increase from 7.08 ± 0.59% to 94.51 ± 1.17% when the biosorbent dosage was set at 3 g/L.

Figure 3 shows the Pb^{2+} biosorption capacity of the studied materials as a function of solution pH. Removal levels were analyzed up to pH 6, as higher pH values resulted in the formation of a precipitate. Precipitation is likely due to the formation of $Pb(OH)_2$, which complicates the evaluation of sorption process efficiency at these pH levels [1, 34, 35].

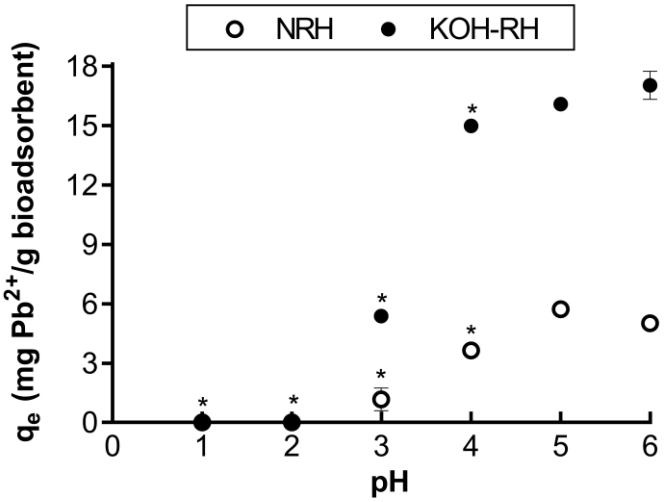

Figure 3 Effect of pH on Pb^{2+} removal by NRH and KOH-RH. Conditions: Time = 1 h, temperature = 20 ± 4°C, $[Pb^{2+}]_0$ = 50 mg/L, biosorbent dosage: NRH = 5 g/L, KOH-RH = 2 g/L. *p < 0.05 vs. the value corresponding to pH = 5.

For the systems analyzed, enhanced metal ion uptake was observed as the solution pH increased to values close to 4-5. At acidic pH, low biosorption could be attributed to the higher concentration and mobility of protons, which preferentially bind to the solid sites [1, 36]. As pH increases, proton concentration decreases while the availability of negatively charged binding sites increases, resulting in enhanced Pb^{2+} sorption [37]. Overall, the highest removal percentages were achieved at a pH close to 5, with sorption capacity (q_e) values of 5.73 ± 0.11 mg/g for NRH and 16.09 ± 0.14 mg/g for KOH-RH.

On the other hand, the maximum Pb^{2+} sorption values for NRH and KOH-RH were obtained at an initial pH (4-5) lower than the pH_{PZC} (6.36 and 7.71). Therefore, electrostatic attractions between biosorbents and Pb^{2+} could not contribute to the sorption as the surfaces of these adsorbents would not be negatively charged at the optimal pH values for the sorption process. However, the pH of the initial solution is not a unique parameter to explain the behavior of metal sorption. Its evolution after contact with the material could affect biosorption through changes in the chemical speciation

of the metal as well as in the surface charge of the adsorbent [32]. In the literature, it has been reported that during sorption, the initial pH may change, creating a suitable environment in which microprecipitation on the surface of the adsorbent could be favored [38]. Furthermore, other mechanisms such as ion exchange, proton displacement, complexation, or chelation could be involved in the observed behavior [39].

Additionally, the effect of contact time (1-180 min) on Pb^{2+} biosorption levels was analyzed (Figure 4).

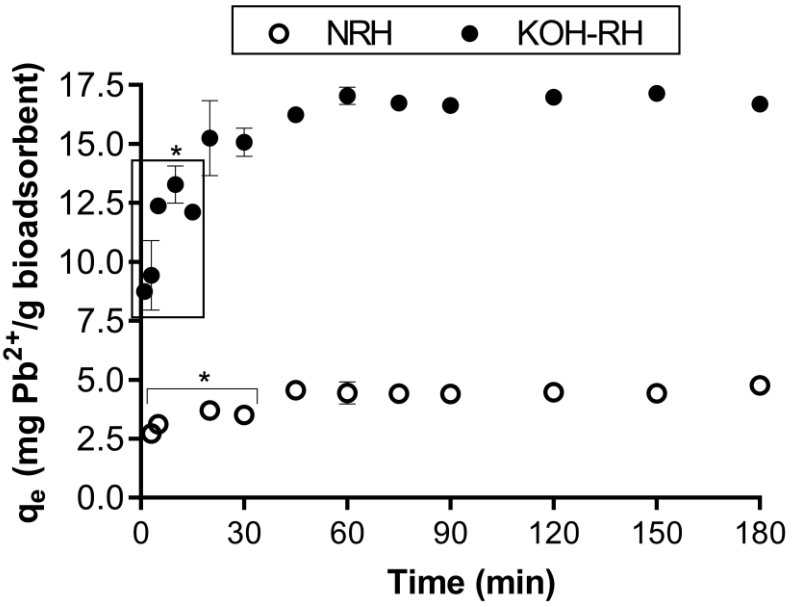

Figure 4 Effect of contact time on Pb^{2+} biosorption by NRH and KOH-RH. Conditions: pH = 5, temperature = 20 ± 4°C, $[Pb^{2+}]_0$ = 50 mg/L, biosorbent dosage: NRH = 5 g/L, KOH-RH = 2 g/L. *$p < 0.05$ vs. the value at 60 min.

The results indicated that biosorption equilibrium was reached after about 30 min. The initially high biosorption rate can be attributed to the abundance of available sorption sites. Over time, the retention rate decreased, likely due to a reduction in the driving force process, which is influenced by both the availability of biosorption sites and the concentration of metal ions in the solution.

The effect of initial metal concentration on removal capacity was investigated in the 10-400 mg/L (Figure 5). As the initial concentration of Pb^{2+} ions increased up to 150 mg/L, an increase in biosorption capacity was observed. However, no further changes in q_e were detected at higher concentrations, likely due to the surface saturation of the biosorbent.

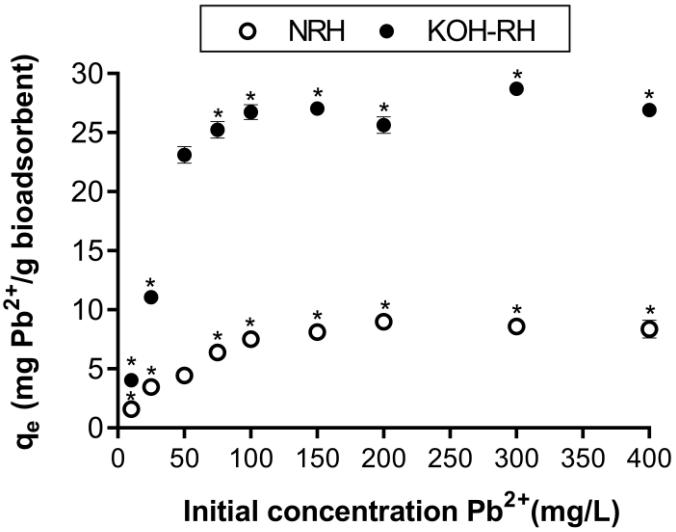

Figure 5 Effect of initial concentration on Pb^{2+} biosorption by NRH and KOH-RH. Conditions: biosorbent dosage: NRH = 5 g/L, KOH-RH = 2 g/L, temperature 20 ± 4°C, pH = 5 and contact time 4 h. *$p < 0.05$ vs. the value corresponding to 50 mg/L.

3.3 Biokinetic Studies

The Lagergren pseudo-first-order and pseudo-second-order equations were used to describe metal uptake by biosorbents [40-42]. Table 1 summarizes the linear form of both models.

Table 1 Linear expressions of pseudo-first-order and pseudo-second-order models.

Model	Linear form	Parameters	Reference
Pseudo-first-order	$log(q_e - q_t) = \log q_e - \frac{k_1}{2.303} t$	t (min): contact time q_e (mg/g): the amount of sorbate adsorbed at equilibrium q_t (mg/g): the amount of sorbate adsorbed at time t k_1 (min^{-1}): rate constant	[43]
Pseudo-second-order	$\frac{1}{q_t} = \frac{1}{q_e} t + \frac{1}{k_2 q_e^2}$	t (min): contact time q_e (mg/g): the amount of sorbate adsorbed at equilibrium q_t (mg/g): the amount of sorbate adsorbed at time t k_2 (g/mg.min): rate constant	[42]

Table 2 presents a summary of the kinetic parameters and correlation coefficients (R^2) obtained by fitting the experimental data to the pseudo-first-order and pseudo-second-order models.

Table 2 Kinetic parameters of pseudo-first-order and pseudo-second-order models for Pb^{2+} removal (50 mg/L) on NRH and KOH-RH at 25°C.

Biosorbent	Pseudo-first order			Pseudo-second order		
	k_1 (min^{-1})	q_e (mg/g)	R^2	k_2 (g/mg.min)	q_e (mg/g)	R^2
NRH	0.014	1.336	0.551	0.039	4.738	0.996
KOH-RH	0.056	7.071	0.970	0.022	17.190	0.999

Based on the correlation coefficients, the kinetics of Pb^{2+} biosorption on the studied systems is better described by the pseudo-second-order model. This approach assumes that the rate-limiting step is chemisorption, involving interactions between the sorbent and the sorbate [42].

3.4 Biosorption Isotherms

To describe the equilibrium behavior of Pb^{2+} ions biosorption on NRH and KOH-RH, the experimental data were fitted to the Langmuir, Freundlich, and Dubinin-Radushkevich isotherms. Mathematical expressions of these models are summarized in Table 3.

Table 3 Non-linear expressions of the isotherm models employed.

Isotherm	Non-linear expression	Parameters	Reference
Langmuir	$q_e = \frac{q_m \cdot b \cdot C_e}{1 + b \cdot C_e}$	q_m (mg/g): monolayer coverage capacity b: Langmuir isotherm constant	[44]
Freundlich	$q_e = K_f \cdot C_e^{\frac{1}{n}}$	K_f (mg/g): Freundlich isotherm constant n: adsorption intensity	[45]
Dubinin-Radushkevich	$q_e = q_{DR} \cdot e^{-K_{DR} \cdot \varepsilon^2}$	q_{DR} (mg/g): maximum amount of M^{2+} uptake on biosorbent K_{DR} (mol^2/J^2): Dubinin-Radushkevich constant ε: Polanyi potential, $\varepsilon = RT \ln(1 + 1/C_e)$; R: gas constant (8.314 J $mol^{-1}K^{-1}$);T: absolute temperature	[46]

Parameters obtained from fitting the data to the three isotherm models are summarized in Table 4. Correlation coefficients indicate that the Langmuir isotherm better describes the equilibrium of the Pb^{2+}-rice husk biosorption system, both in its natural and chemically modified forms (Table 4). This model assumes monolayer sorption on a surface with a finite number of homogeneous and independent sites.

Table 4 Parameters and coefficients of the Langmuir, Freundlich, and Dubinin-Radushkevich isotherms applied to Pb^{2+} biosorption on NRH and KOH-RH.

Biosorbent	Langmuir			Freundlich			Dubinin-Radushkevich			
	q_m (mg/g)	b (L/mg)	R^2	n	K_f	R^2	q_{DR} (mg/g)	K_{DR} (mol^2/J^2)	ε (kJ/mol)	R^2
NRH	8.464	0.093	0.995	3.903	2.184	0.964	6.646	4.7×10^{-8}	3.261	0.684
KOH-RH	27.450	0.614	0.998	4.361	9.224	0.790	25.998	2.8×10^{-7}	1.343	0.961

The maximum sorption capacity values (q_{max}) obtained for the biosorbents studied were compared with those reported in the literature for different types of residues (Table 5). The sorption capacity obtained for the KOH-activated alternative (27.450 mg/g) is comparable to the results reported in the literature. Notably, although some residues exhibit higher q_{max} than those reported in this work, the sorption process was not evaluated under the same operating conditions, making it difficult to directly compare and determine which residue provides better Pb^{2+} retention. Thus, KOH-treated rice husk presents a viable alternative for Pb^{2+} removal from solutions.

Table 5 Comparison of Pb^{2+} removal on rice husk with other adsorbents.

Adsorbent	q_{max} (mg/g)	pH	T (K)	References
Onion skins	200.00	6.00	303	[37]
Raw clay	129.87	6.00	298	[47]
Calcined clay	172.41			
Chicken feathers	55.43	5.00	298	[48]
Almond shells	54.64	6.00	303	[49]
Citrus limetta leaves	62.89	6.00	298	[50]
Bentonite	119.65			
Zeolite	136.99	7.00	298	[51]
Steel slag	55.87			
Sunflower Wood Fly Ash	434.78	7.59	296	[52]
Magnetic cellulose nanocrystals/nylon 6 nanocomposite	18.88	8.00	298	[53]
Almond shells	5.90	5.00	298	[54]
Hazelnut shell	7.30			
Rice husk	8.46	5.00	295	This work
Rice husk-KOH	27.45	5.00	295	This work

3.5 Characterization of Ceramic Pieces

After biosorption experiments, the Pb^{2+}-loaded KOH-RH biosorbent (KOH-RH-Pb^{2+}) and NRH were used as replacements in the ceramic pieces. At the end of the thermal treatment, the products exhibited a homogeneous reddish color due to iron oxide and a well-defined structure without shelling. This presents an advantage from both an aesthetic and a commercial perspective (Figure 6).

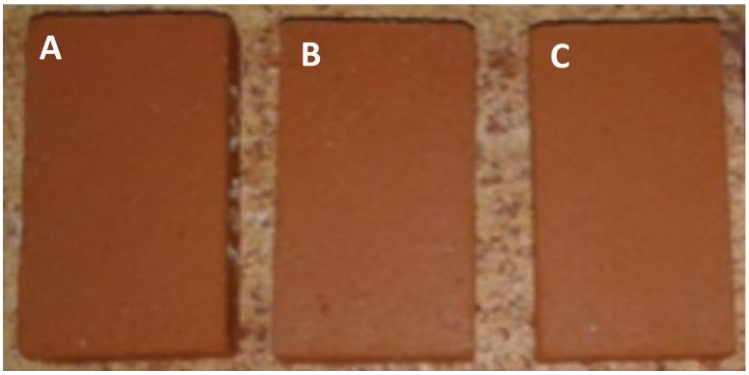

Figure 6 Macroscopic appearance of the obtained bricks. A: commercial clay brick (0% NRH), B: brick with biomass (10% NRH), C: brick with biomass loaded with Pb^{2+} (10% KOH-RH-Pb^{2+}).

In general, samples with 10% biomass content exhibited favorable macroscopic characteristics, with well-preserved edges, corners, and angles. These observations suggest a satisfactory level of sintering, further confirmed through detailed microscopic analyses and the evaluation of physical properties.

The analysis of the obtained products using optical microscopy revealed a high degree of integration between the raw materials. Figure 7 presents micrographs of the ceramic matrices, comparing those derived from the use of commercial clay (0% NRH) with those featuring a 10% biomass replacement (10% KOH-RH-Pb^{2+}). In all cases, homogeneity was observed in the pieces, demonstrating good integration of the mixtures without segregation of specific phases during the firing of the bricks.

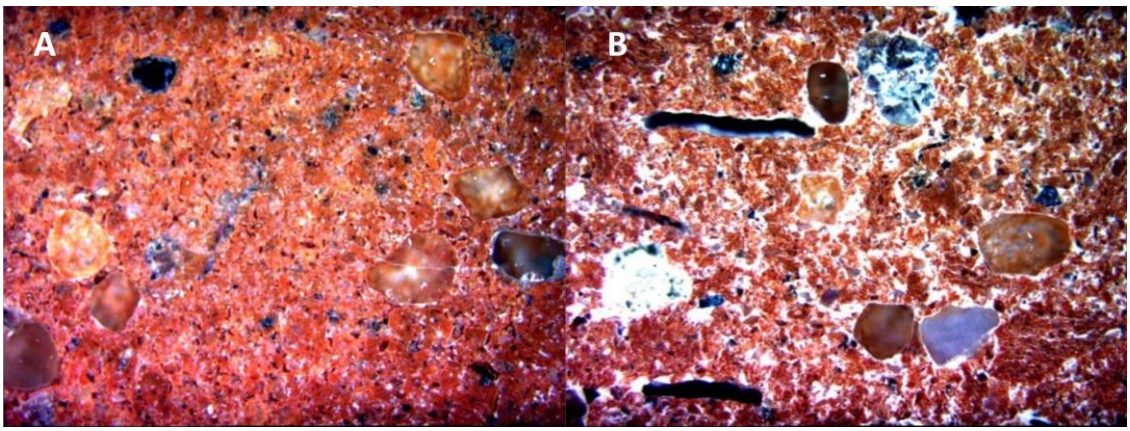

Figure 7 Optical micrographs of ceramic pieces. A: commercial clay brick (0% NRH), B: brick with biomass loaded with Pb^{2+} (10% KOH-RH-Pb^{2+}). Magnification: 50×.

As observed in Figure 7B, the bricks containing added residual biomass exhibited pores in their structure. The pore size (<1 mm) and elongated shape reflect the morphological characteristics of the husk used. This suggests that the sintering process began either before or simultaneously with the combustion of the organic fraction of the husk, thereby preserving the original space occupied by the husk within the brick. Consequently, the resulting porous structure is a direct consequence of this unique sintering-combustion interaction.

Micrographs revealed the presence of silicoaluminates from the raw clay material, appearing as distinct, well-defined particles integrated within the brick matrix. These silicoaluminates were uniformly distributed throughout the pieces.

The properties analyzed in the bricks—porosity, water absorption, MOR, PVV, and LOI—are summarized in Table 6.

Table 6 Physical properties of the ceramic products.

	0% NRH	10% NRH	10% KOH-RH-Pb^{2+}
LOI (%)	5.2	7.2	6.7
PVV (%)	9.9	9.4	9.5
Porosity (%)	21.9	27.3	25.5
Water absorption (%)	10.7	13.6	13.0
MOR (MPa)	8.7	6.3	7.3

It was observed that the incorporation of rice husk decreased the PVV of the pieces, which also exhibited increased porosity. Although a decrease in the modulus of rupture was noted, the obtained values remain within market requirements.

The mechanical characteristics of the ceramic pieces fall within the values established by both the market and the ASTM C410-60 standard for bricks used on industrial floors, which sets a minimum MOR value of 5.2 MPa.

3.6 Immobilization Studies

Ecotoxicity tests were conducted on KOH-RH-Pb^{2+} and ceramic bricks by replacing contaminated husks. The results are presented in Figure 8.

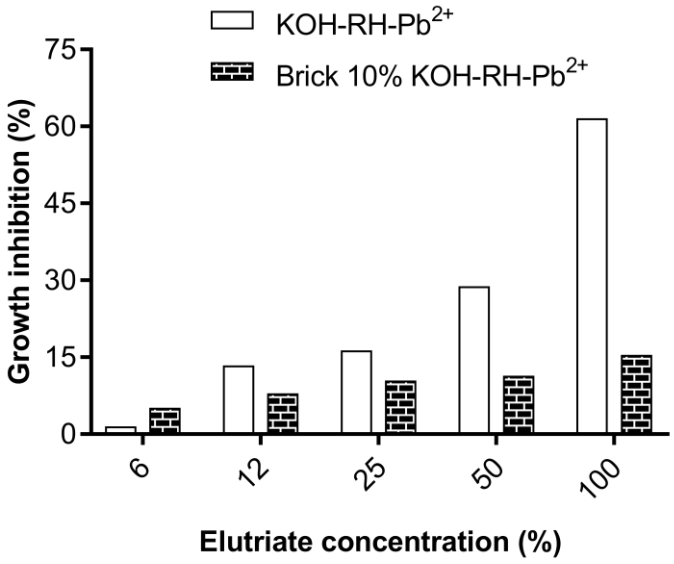

Figure 8 Ecotoxicity analysis of KOH-RH-Pb^{2+} and ceramic brick 10% KOH-RH-Pb^{2+}.

In general, it was observed that the root growth inhibition percentages for the loaded bricks were significantly lower than those for the contaminated husk, within the range of elutriate concentrations studied.

On the other hand, the analysis of leachates from the ceramic pieces containing contaminated husk was performed using atomic absorption spectroscopy. The values obtained were below the detection limit of the method, indicating that the Pb^{2+} levels in the leachate are lower than those established by current regulations.

The results of ecotoxicity and leaching tests conducted on the final products suggest that incorporating Pb^{2+}-loaded rice husk into ceramic matrices is a feasible method for immobilizing the contaminant within the structure.

4. Conclusions

In this study, the optimization of physicochemical parameters involved in Pb^{2+} removal using natural and chemically modified rice husk was performed. Alkaline treatment of rice husk significantly improved metal retention, reaching biosorption levels close to 95% at a biosorbent dosage of 3 g/L. The optimal pH for the process was 5, and equilibrium was achieved within 30 min. The equilibrium data were fitted to different theoretical models, with the Langmuir isotherm providing the best fit to describe Pb^{2+} biosorption onto the employed biosorbents. Kinetic studies demonstrated that the pseudo-second-order model provided the best correlation with the experimental data for the analyzed systems.

After biosorption, the feasibility of incorporating Pb^{2+}-loaded rice husk into clay ceramic matrices to immobilize the toxic metal was evaluated. The results suggest that the ceramic pieces successfully immobilized the Pb^{2+} within their structure. Additionally, they exhibited a well-defined structure without shelling, a homogeneous color, sharp edges, a reasonable degree of sintering, and properties suitable for practical use.

Acknowledgments

The authors would like to express their gratitude to the INTEMA, Argentina, for conducting the raw materials characterization tests, and to the UTN for the financial support provided for this work. Special thanks are also extended to the GEA, UTN-FRSN, for their contribution to the characterization of the ceramic pieces.

Author Contributions

MR conducted the experimental work, processed the data, and wrote the manuscript. VC contributed to the experimental work, participated in the discussion of the results, and helped write the manuscript. EC assisted with the experimental work. RA participated in the discussion of the results. MG coordinated the research and wrote the manuscript. All authors read and approved the final manuscript.

Funding

This work was supported by UTN.

Competing Interests

The authors declare that they have no known financial or personal conflicts of interest that could have influenced the work reported in this paper.

References

1. Neskoromnaya EA, Khamizov RK, Melezhyk AV, Memetova AE, Mkrtchan ES, Babkin AV. Adsorption of lead ions (Pb^{2+}) from wastewater using effective nanocomposite GO/CMC/FeNPs: Kinetic, isotherm, and desorption studies. Colloids Surf A Physicochem Eng Asp. 2022; 655: 130224.
2. Chen WH, Hoang AT, Nižetić S, Pandey A, Cheng CK, Luque R, et al. Biomass-derived biochar: From production to application in removing heavy metal-contaminated water. Process Saf Environ Prot. 2022; 160: 704-733.
3. Vakili M, Deng S, Cagnetta G, Wang W, Meng P, Liu D, et al. Regeneration of chitosan-based adsorbents used in heavy metal adsorption: A review. Sep Purif Technol. 2019; 224: 373-387.
4. Tseveendorj E, Enkhdul T, Lin S, Dorj D, Oyungerel S, Soyol-Erdene TO. Biosorption of lead (II) from an aqueous solution using biosorbents prepared from water plants. Mong J Chem. 2017; 18: 52-61.
5. Verma M, Ahmad W, Park JH, Kumar V, Vlaskin MS, Vaya D, et al. One-step functionalization of chitosan using EDTA: Kinetics and isotherms modeling for multiple heavy metals adsorption and their mechanism. J Water Process Eng. 2022; 49: 102989.
6. Zamora-Ledezma C, Negrete-Bolagay D, Figueroa F, Zamora-Ledezma E, Ni M, Alexis F, et al. Heavy metal water pollution: A fresh look about hazards, novel and conventional remediation methods. Environ Technol Innov. 2021; 22: 101504.
7. Mitra S, Chakraborty AJ, Tareq AM, Emran T, Nainu F, Khusro A, et al. Impact of heavy metals on the environment and human health: Novel therapeutic insights to counter the toxicity. J King Saud Univ Sci. 2022; 34: 101865.
8. Jaishankar M, Tseten T, Anbalagan N, Mathew BB, Beeregowda KN. Toxicity, mechanism and health effects of some heavy metals. Interdiscip Toxicol. 2014; 7: 60-72.
9. Jan AT, Azam M, Siddiqui K, Ali A, Choi I, Haq QM. Heavy metals and human health: Mechanistic insight into toxicity and counter defense system of antioxidants. Int J Mol Sci. 2015; 16: 29592-29630.
10. Naiya TK, Bhattacharya AK, Mandal S, Das SK. The sorption of lead (II) ions on rice husk ash. J Hazard Mater. 2009; 163: 1254-1264.
11. Samuel MS, Shah SS, Bhattacharya J, Subramaniam K, Singh NP. Adsorption of Pb (II) from aqueous solution using a magnetic chitosan/graphene oxide composite and its toxicity studies. Int J Biol Macromol. 2018; 115: 1142-1150.
12. Tchounwou PB, Yedjou CG, Patlolla AK, Sutton DJ. Heavy metals toxicity and the environment. In: Molecular, clinical and environmental toxicology. Basel: Springer; 2012. pp. 133-164.
13. Azcona-Cruz MI, Ramírez-Ayala R, Vicente-Flores G. Efectos tóxicos del plomo. Rev Espec Méd Quirúrg. 2015; 20: 72-77.
14. Barakat MA. New trends in removing heavy metals from industrial wastewater. Arab J Chem. 2011; 4: 361-377.

15. Carolin CF, Kumar PS, Saravanan A, Joshiba GJ, Naushad M. Efficient techniques for the removal of toxic heavy metals from aquatic environment: A review. J Environ Chem Eng. 2017; 5: 2782-2799.
16. Deng Y, Zhao R. Advanced Oxidation Processes (AOPs) in wastewater treatment. Curr Pollut Rep. 2015; 1: 167-176.
17. Naja GM, Volesky B. Metals in the environment: Toxicity and sources. In: Heavy metals in the environment. Humana Press; 2009. pp. 13-62.
18. Nishat A, Yusuf M, Qadir A, Ezaier Y, Vambol V, Ijaz Khan M, et al. Wastewater treatment: A short assessment on available techniques. Alex Eng J. 2023; 76: 505-516.
19. Beni AA, Esmaeili A. Biosorption, an efficient method for removing heavy metals from industrial effluents: A Review. Environ Technol Innov. 2020; 17: 100503.
20. Park D, Yun YS, Park JM. The past, present, and future trends of biosorption. Biotechnol Bioprocess Eng. 2010; 15: 86-102.
21. Abdolali A, Ngo HH, Guo W, Zhou JL, Zhang J, Liang S, et al. Application of a breakthrough biosorbent for removing heavy metals from synthetic and real wastewaters in a lab-scale continuous fixed-bed column. Bioresour Technol. 2017; 229: 78-87.
22. Ali RM, Hamad HA, Hussein MM, Malash GF. Potential of using green adsorbent of heavy metal removal from aqueous solutions: Adsorption kinetics, isotherm, thermodynamic, mechanism and economic analysis. Ecol Eng. 2016; 91: 317-332.
23. Luzardo FH, Velasco FG, Alves CP, Correia IK, Cazorla LL. Chemical characterization of agroforestry solid residues aiming its utilization as adsorbents for metals in water. Rev Bras Eng Agric Ambient. 2015; 19: 77-83.
24. Neris JB, Luzardo FH, da Silva EG, Velasco FG. Evaluation of adsorption processes of metal ions in multi-element aqueous systems by lignocellulosic adsorbents applying different isotherms: A critical review. Chem Eng J. 2019; 357: 404-420.
25. Mo J, Yang Q, Zhang N, Zhang W, Zheng Y, Zhang Z. A review on agro-industrial waste (AIW) derived adsorbents for water and wastewater treatment. J Environ Manag. 2018; 227: 395-405.
26. Lata S, Samadder SR. Removal of heavy metals using rice husk: A review. Int J Environ Sci Dev. 2014; 4: 165-170.
27. Shamsollahi Z, Partovinia A. Recent advances on pollutants removal by rice husk as a bio-based adsorbent: A critical review. J Environ Manag. 2019; 246: 314-323.
28. Naik RL, Rupas Kumar M, Bala Narsaiah T. Removal of heavy metals (Cu & Ni) from wastewater using rice husk and orange peel as adsorbents. Mater Today Proc. 2023; 72: 92-98.
29. Romano M, Pelozo G, Quaranta N, Corne V, García MC. Ceramic matrices for immobilization of heavy metals adsorbed on rice husk. SN Appl Sci. 2020; 2: 964.
30. Quaranta N, Caligaris M, Pelozo G, Césari A, Cristóbal A. Use of waste from the peanut industry in the manufacture of building materials. Int J Sustain Dev Plan. 2018; 13: 662-670.
31. Simón D, Quaranta N, Medici S, Costas A, Cristóbal A. Immobilization of Zn (II) ions from contaminated biomass using ceramic matrices. J Hazard Mater. 2019; 373: 687-697.
32. Fiol N, Villaescusa I. Determination of sorbent point zero charge: Usefulness in sorption studies. Environ Chem Lett. 2009; 7: 79-84.
33. Pelozo G, Quaranta N, Caligaris M, Romano M, Cristóbal A. Effect of the incorporation of biomass wastes on the properties of fired clay bricks. Proceedings of the 33rd International

Conference on Solid Waste Technology and Management; 2018 March 11-14; Washington, D.C., USA. Chester, PA: Widener University.
34. Adebowale KO, Unuabonah IE, Olu-Owolabi BI. The effect of some operating variables on the adsorption of lead and cadmium ions on kaolinite clay. J Hazard Mater. 2006; 134: 130-139.
35. Gupta S, Bhattacharyya KG. Adsorption of Ni (II) on clays. J Colloid Interface Sci. 2006; 295: 21-32.
36. Annadurai G, Juang RS, Lee DJ. Use of cellulose-based wastes for adsorption of dyes from aqueous solutions. J Hazard Mater. 2002; 92: 263-274.
37. Saka C, Şahin Ö, Demir H, Kahyaoğlu M. Removal of lead (II) from aqueous solutions using pre-boiled and formaldehyde-treated onion skins as a new adsorbent. Sep Sci Technol. 2011; 46: 507-517.
38. Taty-Costodes VC, Fauduet H, Porte C, Delacroix A. Removal of Cd (II) and Pb (II) ions, from aqueous solutions, by adsorption onto sawdust of Pinus sylvestris. J Hazard Mater. 2003; 105: 121-142.
39. Michalak I, Chojnacka K, Witek-Krowiak A. State of the art for the biosorption process—A review. Appl Biochem Biotechnol. 2013; 170: 1389-1416.
40. Asuquo E, Martin A, Nzerem P, Siperstein F, Fan X. Adsorption of Cd (II) and Pb (II) ions from aqueous solutions using mesoporous activated carbon adsorbent: Equilibrium, kinetics and characterisation studies. J Environ Chem Eng. 2017; 5: 679-698.
41. Chen Y, Wang H, Zhao W, Huang S. Four different kinds of peels as adsorbents for the removal of Cd (II) from aqueous solution: Kinetics, isotherm and mechanism. J Taiwan Inst Chem Eng. 2018; 88: 146-151.
42. Ho YS, McKay G. Pseudo-second order model for sorption processes. Process Biochem. 1999; 34: 451-465.
43. Lagergren S. Zur theorie der sogenannten adsorption geloster stoffe. K Sven Vetenskapsakad Handl. 1898; 24: 1-39.
44. Langmuir I. The adsorption of gases on plane surfaces of glass, mica and platinum. J Am Chem Soc. 1918; 40: 1361-1403.
45. Freundlich HM. Concerning adsorption in solutions. Z Phys Chem. 1906; 57: 385-470.
46. Dubinin MM, Radushkevich LV. Equation of the characteristic curve of activated charcoal. Proc Calif Acad Sci. 1947; 55:331-333.
47. Teğin I, Batur MS, Yavuz Ö, Saka C. Removal of Cu (II), Pb (II) and Cd (II) metal ions with modified clay composite: Kinetics, isotherms and thermodynamics studies. Int J Environ Sci Technol. 2023; 20: 1341-1356.
48. Chen H, Li W, Wang J, Xu H, Liu Y, Zhang Z, et al. Adsorption of cadmium and lead ions by phosphoric acid-modified biochar generated from chicken feather: Selective adsorption and influence of dissolved organic matter. Bioresour Technol. 2019; 292: 121948.
49. Kahvecioğlu K, Teğin İ, Yavuz Ö, Saka C. Phosphorus and oxygen co-doped carbon particles based on almond shells with hydrothermal and microwave irradiation process for adsorption of lead (II) and cadmium (II). Environ Sci Pollut Res. 2023; 30: 37946-37960.
50. Aboli E, Jafari D, Esmaeili H. Heavy metal ions (lead, cobalt, and nickel) biosorption from aqueous solution onto activated carbon prepared from *Citrus limetta* leaves. Carbon Lett. 2020; 30: 683-698.

51. Pfeifer A, Škerget M, Čolnik M. Removal of iron, copper, and lead from aqueous solutions with zeolite, bentonite, and steel slag. Sep Sci Technol. 2020; 56: 2989-3000.
52. Kalak T, Cierpiszewski R, Ulewicz M. High efficiency of the removal process of Pb (II) and Cu (II) ions with the use of fly ash from incineration of sunflower and wood waste using the CFBC technology. Energies. 2021; 14: 1771.
53. Suter E, Rutto H, Kohitlhetse I. Adsorptive removal of Pb^{2+} from aqueous solution by magnetic biodegradable and polymeric cellulose/Nylon 6@Fe_3O_4 nanocomposite encapsulated with chitosan. Desalin Water Treat. 2024; 320: 100782.
54. Cataldo S, Gianguzza A, Milea D, Muratone N, Pettignano A, Sammartano S. A critical approach to the toxic metal ion removal by hazelnut and almond shells. Environ Sci Pollut Res. 2019; 25: 4238-4253.